Comparative bending dynamics in DNA with and without regularly repeated adenine tracts

Alexey K. Mazur*
Laboratoire de Biochimie Théorique, CNRS UPR9080, Institut de Biologie Physico-Chimique, 13, Rue Pierre et Marie Curie, Paris, 75005, France

Dimitri E. Kamashev†
Laboratoire de Physiologie Bectérienne, CNRS UPR9073, Institut de Biologie Physico-Chimique, 13, Rue Pierre et Marie Curie, Paris, 75005, France

(Received 11 January 2002; published 29 July 2002)

The macroscopic curvature of double helical DNA induced by regularly repeated adenine tracts is well known but still puzzling. Its physical origin remains controversial even though it is perhaps the best-documented sequence modulation of DNA structure. The paper reports on comparative theoretical and experimental studies of bending dynamics in 35-mer DNA fragments. This length appears large enough for the curvature to be distinguished by gel electrophoresis. Two DNA fragments, with identical base pair composition but different sequences, are compared. In the first one, a single A-tract motif is four times repeated in phase with the helical screw whereas the second sequence is ''random.'' Both calculations and experiments indicate that the A-tract DNA is distinguished by large static curvature and characteristic bending dynamics, suggesting that the computed effect corresponds to the experimental phenomenon. The results agree poorly with the view that DNA bending is caused by the specific local geometry of base pair stacking or binding of solvent counterions, but lend additional support to the hypothesis of a compressed frustrated state of the backbone as the principal physical cause of the static curvature. Possible ways of experimental verification of this hypothesis are discussed.

DOI: 10.1103/PhysRevE.66.011917 PACS number(s): 87.14.Gg

I. INTRODUCTION

It is generally accepted that the base pair sequence can affect the overall form of the DNA double helix. Intrinsic DNA bending is the simplest such effect. Natural static curvature was discovered nearly 20 years ago in DNA containing regular repeats of A_nT_m, with $n+m>3$, called A tracts [1–3]. Since then this intriguing phenomenon has been actively studied, with several profound reviews of the results published in different years [4–9]. It is known that the curvature is directed toward the minor grooves of the A tracts and/or the major grooves of the junction zones between them, and that its magnitude is around 18° per A tract. However, the exact sites and the character of local bends remain a matter of debate as well as their mechanism and physical origin.

The pioneering conformational calculations of the 1970s already showed that the DNA double helix exhibits significant bendability, which is anisotropic and sequence dependent [10,11]. Based upon these views the wedge model offered the very first explanation of bending induced by A tracts by postulating that stacking in ApA steps is intrinsically nonparallel [12]. Modified versions of this theory accounted for a substantial part of available experimental data, with good scores of curvature prediction from sets of fitted wedge angles [13–15]. At the same time, clear experimental counterexamples exist where bending could not result from simple accumulation of wedges [16,17]. The junction model [2,18] explained experimental data on gel retardation of curved DNA better than other theories. It originated from the idea that a bend should occur when two different DNA forms are stacked [19]. If the poly-dA double helix has a special B′ form as suggested by some data [20] the helical axis should be kinked when an A tract is interrupted by a random sequence. In turn, the x-ray data are best interpreted with an alternative theory that postulates that bending is intrinsic in most DNA sequences except A tracts, which are straight [21–23]. Another interesting model has attracted attention in the recent years, namely, bending by electrostatic forces that result from neutralization of phosphates by solvent cations trapped in the minor grooves of A tracts [24]. This problem is of general importance because the accumulated large volume of apparently paradoxical observations suggests that some important factors are still unknown that may be essential for understanding the fine structure and the biological function of the DNA molecule.

Recently, a different hypothesis has been proposed for the physical origin of intrinsic bends in double helical DNA [25]. According to it, the sugar-phosphate backbone in physiological conditions is slightly compressed, that is, the equilibrium specific length of the corresponding free polymer in the same solvent is larger than that in the canonical B form. Therefore, the backbone ''pushes'' stacked base pairs, forcing them to increase the helical twist and rise, while the stacking interactions oppose this. As a result, the backbone increases its length by deviating from its regular spiral trace on the cylindrical surface of the double helix, which causes quasisinusoidal modulations of the DNA grooves. Concomitant base stacking perturbations result in macroscopic static

*FAX: +33[0]1.58.41.50.26. Electronic address: alexey@ibpc.fr
†Present address: CNRS UPR9051, Hôpital St. Lois, 1 av. C. Vellefaux, 75475 Paris Cedex 10, France.

 ©2002 The American Physical Society

curvature when the period of these modulations corresponds to an integral number of helical turns, while its phase is fixed due to regular alternation of certain properties of base pairs along the sequence.

Drew and Travers [26,27] apparently were the first to notice that narrowing of both DNA grooves at the inner edge of a bend is a necessary and sufficient condition of bending, and that an unusual local groove width should be accompanied by structural perturbations beyond this region. They, and later Burkhoff and Tullius [28], considered the preference of narrow and wide minor groove profiles by certain sequences as the possible original cause of this effect. Sprous *et al.* [29] proposed a similar idea within the context of the junction model. In a certain sense, the compressed backbone theory continues the same line of thinking. It offers a consistent interpretation to many intriguing experimental observations concerning the A-tract curvature and we will discuss its main aspects in more detail later.

Conformational modeling earlier helped to shed light upon many aspects of the above problems. Construction of spatial DNA traces from local wedge parameters combined with Monte Carlo simulations of loop closure was applied to check different hypotheses and to estimate local bending angles from experimental data [18,30]. Energy calculations revealed that bending may be easier at some dinucleotide steps and in certain specific directions [11,31], with experimental sequence effects reproduced in some remarkable examples [32]. DNA was shown to have local energy minima in bent conformations corresponding to the junction model [33,34]. All atom Monte Carlo calculations showed that narrowing of the A-tract minor groove with a few NMR-derived restraints may be sufficient to provoke the curvature [35].

The simplest setup for modeling DNA bending is to take a straight symmetrical double helix and let it bend spontaneously with no extra forces applied, that is, due to generic atom-atom interactions. This ''naive'' approach has recently become possible owing to the progress in methodology of molecular dynamics (MD) calculations of nucleic acids [36], which was demonstrated by successful simulations of several curved and straight DNA fragments in realistic environments including explicitly water and counterions [29,37]. The character of bending qualitatively agreed with the theories outlined above so that none of them could be preferred. Thorough discriminative testing would require more extensive sampling of bending events, which should become possible in future. Detailed structures of short A-tract fragments have also been studied by MD [38,39].

The major obstacle in free MD simulations of intrinsic curvature is the limited capacity for sampling of bending events. The physical time of transition between straight and bent conformations may be too long for a statistically significant number of such events to be accumulated in simulations. Moreover, experimental effects may not appear during infinitely long MD simulations because models are never perfect. To circumvent these difficulties, we employed a different strategy. We first looked for, and found, a short A-tract motif that could reproducibly induce stable bends in DNA during a few nanoseconds of MD with a simplified model of B-DNA. We used this motif to construct longer double helices with intrinsic curvature *in silico* and we could increase the length of DNA fragments in calculations to 35 base pairs (bp), which makes possible a direct comparison with experiments *in vitro*.

The two 35-mer DNA fragments we study here have identical base pair composition and differ only in their sequences. The first fragment is the designed A-tract repeat while the other sequence is ''random.'' All MD trajectories start from canonical straight A- and B-DNA conformations. For the A-tract DNA fragment they converged to a single statically bent state with planar curvature toward the narrowed minor grooves at the 3′ ends of A tracts. The magnitude of bending is close to the experimental estimates. The random fragment was also not straight, but its curvature was much less significant and less planar. In gel migration assays the two molecules produce well-resolved distinct bands, with the A-tract sequence demonstrating a reduced mobility characteristic of curved DNA. These results suggest that the intrinsic DNA curvature reproduced in calculations corresponds to the experimental phenomenon. The bending dynamics qualitatively agrees with the compressed backbone theory, but it cannot be accounted for by other models.

II. MATERIALS AND METHODS

A. Calculations

Molecular dynamics simulations have been performed by the internal coordinate method (ICMD) [40,41] including special technique for flexible sugar rings [42], with AMBER94 [43,44] force field and TIP3P water [45]. All calculations were carried out without cutoffs and boundary conditions. The time step was 10 fs. The so-called minimal model of B-DNA was used [46,47]. It includes only a partial hydration shell and treats counterion and long range solvation effects implicitly by reducing phosphate charges to -0.5 and applying linear scaling of Coulomb forces. These rough empirical approximations result in an unusually good agreement of computed conformations with experimental data, which cannot be obtained with other methods currently available. The advantages as well as the limitations of this approach have been reviewed [36]. For qualitative analysis of DNA bending it is most important that the model has no other bias toward bent or nonbent conformations except the base pair sequence.

The two 35 bp DNA fragments are referred to below as At and nAt, for the A-tract repeat and the non-A-tract DNA, respectively. For both fragments two long MD trajectories were computed starting from either A or B canonical DNA forms. These four trajectories are referred to as At-A, At-B, nAt-A, and nAt-B, respectively, where the last character indicates the starting state. The starting fiber A- and B-DNA models were constructed from the published atom coordinates [48]. Our hydration protocol [25] fills only the minor DNA groove and generally places fewer water molecules around the A form. For better comparison the number of water molecules in At-A and nAt-A is increased after equilibration to those in At-B and nAt-B, respectively. All trajectories were continued to 20 ns except At-B, which was stopped at about 12 ns because it had clearly converged long

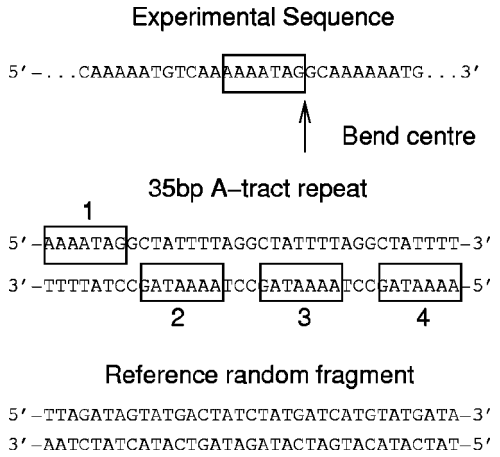

FIG. 1. Construction of 35 bp double stranded DNA fragments. The top sequence with the boxed heptamer motif AAAATAG is taken from the trypanosome kinetoplast DNA [2]. The A tracts are numbered and their centers are separated by approximately 10 bp. The reference random fragment has the same base pair content as the 35-mer repeat, but its sequence has been manually reshuffled to exclude any A-tract motifs.

before. The programs CURVES [49], XMMOL [50], and MATHEMATICA by Wolfram Research Inc. were employed for graphics and data analysis.

B. Oligonucleotides and construction of 5′-labeled DNA probes

The sequences of the 35 nucleotide long synthetic oligonucleotides used here are shown in Fig. 1. The double stranded DNA molecules were obtained by annealing of the two complementary oligonucleotides, one of them labeled with T4 polynucleotide kinase and [^{32}P]-ATP. The annealing was carried out by incubating the oligonucleotides (300 nM) for 3 min at 80 °C in 20 mM tris (hydroxymethyl)-aminomethane (Tris)-HCl (*p*H 8.0), 400 mM NaCl, and 0.2 mM ethylenediaminetetra-acetic acid (EDTA) and then allowing them to cool slowly.

C. Gel mobility assays

Mobility of the DNA fragments was analyzed in 16% gels (acrylamide to bis-acrylamide, 29:1) buffered with 90 mM Tris-borate and 1 mM EDTA, pH 8.6. Gels were prerun under constant power until stabilization of current. End-labeled DNA in a buffer containing 20 mM Tris-HCL, 50 mM NaCL, and 7% glycerol, pH 8.0, and bromophenol-blue was loaded onto the gel. The electrophoresis was performed under constant power and constant temperature of 8 °C. The dried gels were exposed to storage phosphor screens and visualized on a 400S PhosphorImager (Molecular Dynamics).

III. RESULTS AND DISCUSSION

A. Construction of DNA fragments

Figure 1 explains how the two DNA fragments used in our study were constructed. The A-tract motif AAAATAG originally attracted our attention in MD simulations of the natural DNA shown in Fig. 1 [51], which is the first curved DNA locus studied *in vitro* [2]. The 35 bp A-tract fragment was constructed by repeating this motif four times and it had to be inverted to make the two DNA termini symmetrical. Such inversion should not affect bending [52], but is essential for simulations because the 3′- and 5′-end A tracts may represent qualitatively different boundaries. In repeated simulations with this and similar A-tract fragments, the static curvature emerged spontaneously and it became more evident as the chain length increased [25]. To obtain a reference non-A-tract DNA, we have manually re-shuffled base pairs of the A-tract repeat. We preferred this randomized sequence to commonly used GC-rich straight fragments in order to keep the base pair content identical and reduce the noise that could cause small variations in gel mobility and hide the subtle differences we were going to detect.

TABLE I. Some structural parameters of standard and computed DNA conformations. The helicoidals are the sequence averaged values computed with the program CURVES [49]. All distances are in angströms and angles in degrees.

	*X*disp	Inclination	Rise	Twist	rmsd vs A-DNA	rmsd vs B-DNA
A-DNA	-5.4	+19.1	2.6	32.7	0.0	10.7
B-DNA	-0.7	-6.0	3.4	36.0	10.7	0.0
At-A	+0.1	-4.0	3.5	34.2	11.6	5.9
At-B	-0.4	-5.2	3.5	34.5	11.6	6.8
nAt-A	-0.1	-4.2	3.5	34.3	10.6	3.8
nAt-B	-0.1	-4.7	3.5	34.4	11.2	4.1

B. Spontaneous development of curvature in simulations

All four trajectories exhibited stable dynamics with DNA structures close to the B form. Table I shows parameters of the final 1 ns average conformations. They all have remarkably similar helicoidals corresponding to a typical B-DNA. For example, the average helical twist estimated from the best-fit B-DNA experimental values [53] gives $(34.0 \pm 0.2)°$ and $(33.8 \pm 0.2)°$ for the A-tract fragment and the randomized sequence, respectively. At the same time, the rms deviations (rmsd) from the canonical structures vary more significantly.

As shown in Fig. 2, during the first few nanoseconds, the rmsd from the canonical B-DNA quickly leveled at around 4 Å in all four trajectories. For the A-DNA start this corresponds to a rapid transition to B form with reduction of rmsd from the initial 10.7 Å. The subsequent dynamics is remarkably different for the At and nAt trajectories. In At-A and At-B, after some delay, the rmsd value drastically increased and stabilized at a higher level of around 6 Å. The traces of the bend angle and the axis shortening indicate that this was a transition to a significantly larger curvature. In contrast, for nAt trajectories, Fig. 2 exhibits only fluctuations at roughly the same level as in At-A and At-B before the transition. The origin of this difference is analyzed in Fig. 3. It displays dynamics of the overall DNA shape by using two orthogonal projections of the helical axis. A planar bend would give a

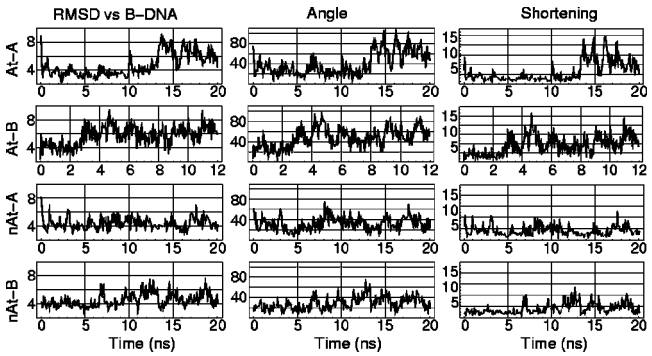

FIG. 2. The time variation of some parameters that characterize the overall DNA shape. The plates are grouped in rows for the same trajectory and in columns for the same parameter. The first column displays the nonhydrogen atom rmsd (in angströms) from the fiber canonical B-DNA [48]. The second column shows the bend angle in degrees. The last column shows the shortening, that is, the excess length of the curved DNA axis with respect to its end-to-end distance. For example, 10% shortening means that the end-to-end distance is 10% shorter than the curved trace. The traces were smoothed by averaging with a window of 75 ps in At-B and 150 ps otherwise.

plane in the **Y** projection and a curved surface in the **X** projection. A sharp increase of curvature in At-A after the 13th nanosecond is evident. Analogous event occurred in At-B after about 3 ns. In agreement with Fig. 2, the two nAt surfaces show fluctuations with amplitudes similar to those during the first 13 ns of At-A. This pattern probably corresponds to a generic type of dynamics characteristic of arbitrary 35-mer DNA fragments.

Comparison of the three columns of plots in Fig. 2 indicates that fluctuations usually occurred simultaneously in all three parameters, which means that the bending dynamics makes a major contribution to the rmsd from B-DNA. Its values shown in Table I are actually much larger than they would be for straight conformations with the same helical parameters. For instance, the rmsd between the At-A and At-B structures in Table I was 2.3 Å only because, as we show below, they were bent in the same direction.

C. Convergence of trajectories

A DNA molecule with detectable static curvature either can have a minimum of potential energy in a bent state or its energy valley should have a special shape such that a bent form has larger conformational entropy [54]. In both cases this state represents a free energy minimum where MD trajectories should be trapped. The question is, however, how

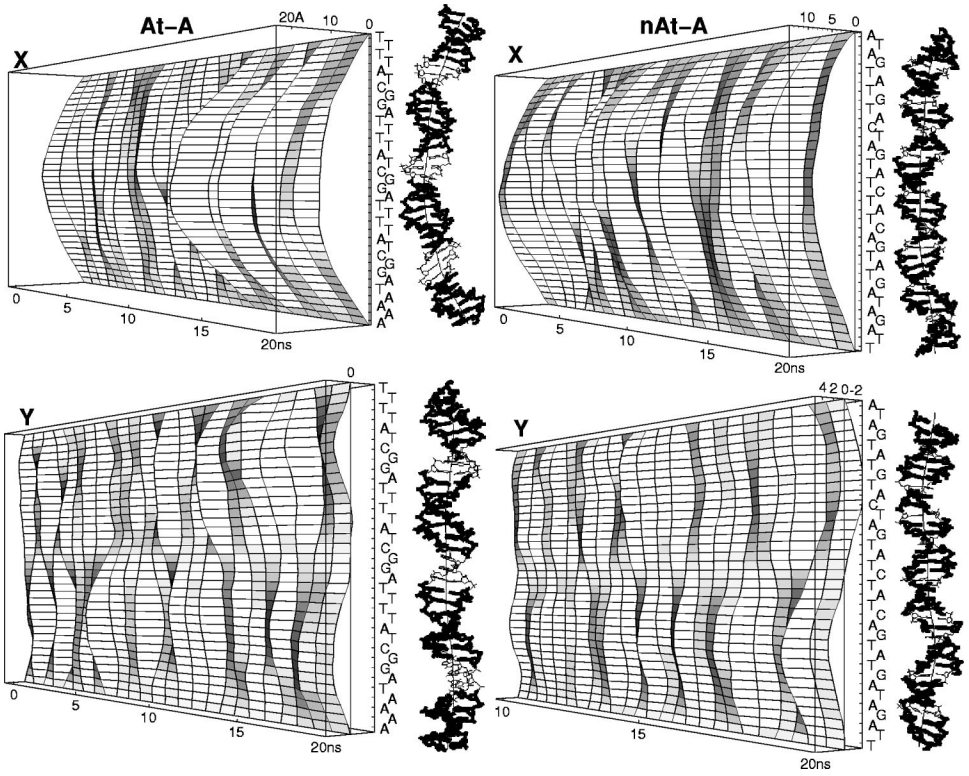

FIG. 3. The time evolution of the overall shape of the helical axis in At-A and nAt-A. The axis of the curved double helix is computed as the best fit common axis of coaxial cylindrical surfaces passing through sugar atoms, which gives solutions close to those produced by the CURVES algorithm [49]. The two surface plots labeled **X** and **Y** are constructed by using projections of the curved axis upon the *XOZ* and *YOZ* planes, respectively, of the global Cartesian frame shown in Fig. 4(a). Any time section of these surfaces gives the corresponding projection averaged over a time window of 400 ps. The horizontal deviation is given in angströms and, for clarity, its relative scale is two times increased with respect to the true DNA length. Shown on the right are the corresponding views of the final 1 ns average conformations. The AT base pairs are shown by thicker lines.

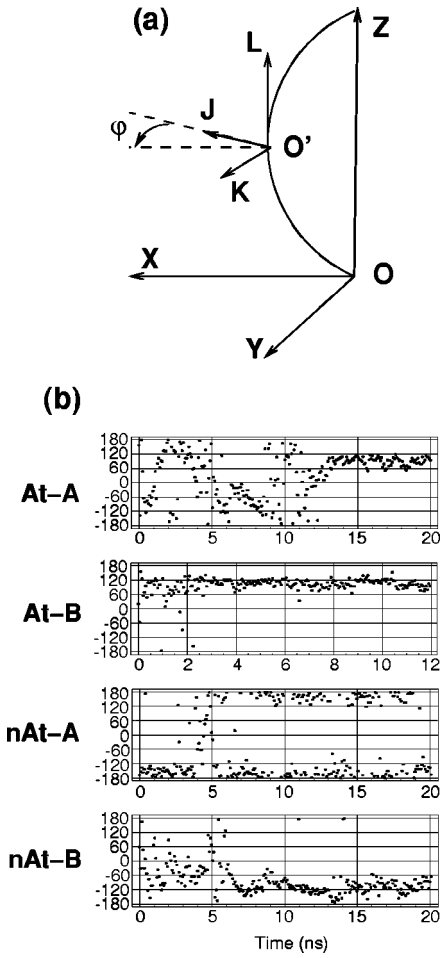

FIG. 4. (a) Geometric constructions used for evaluating the DNA bending. The two coordinate frames shown are the global Cartesian coordinates $(OXYZ)$, and the local frame constructed in the middle point of the curved DNA axis according to the Cambridge convention $(O'JKL)$ [94]. The curve is rotated with its two ends fixed at the Z axis to put the middle point in the plane XOZ. The bending direction is measured by the angle φ between this plane and the vector **J** of the local frame. By definition, this vector points to the major DNA groove along the short axis of the reference base pair [94]. Consequently, the zero φ value corresponds to the overall bend toward the minor groove in the middle of the DNA fragment as in the very first analyses of local DNA curvature [11]. (b) The time evolution of the bending direction as measured by the φ angle in plate (a) (in degrees). The traces have been smoothed by averaging with a window of 75 ps in At-B and 150 ps otherwise.

long a real MD trajectory should stay in a bent conformation to be representative. Some experiments suggest that bending dynamics in DNA fragments of only 100 base pairs may involve relaxation times longer than a microsecond [55,56]; therefore, no practical procedure exists to prove rigorously that computed conformations are representative. Nevertheless, if several trajectories converge to the same state from very different starting points, one can argue that this state is an attractor in the conformational space, which is a necessary condition of the static curvature. The reciprocal convergence of trajectories starting from canonical A- and B-DNA, therefore, is a very important aspect of these simulations. These

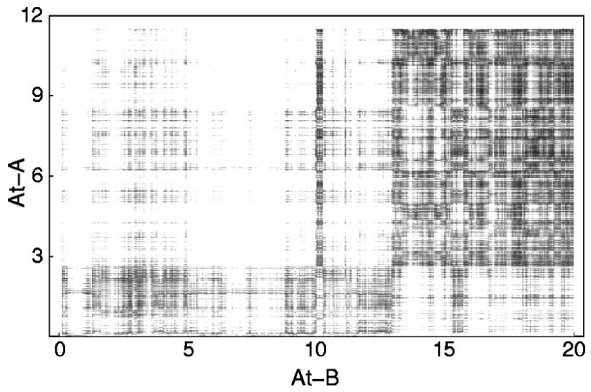

FIG. 5. A two-dimensional (2D) density plot of the rms difference between At-A and At-B. Conformations spaced by 2.5 ps intervals were first averaged over 50 and 25 ps intervals in At-A and At-B, respectively, and the resulting structures compared between the trajectories. Darker shading implies smaller rmsd values. The lower left corner corresponds to the initial structures, that is, the canonical A and B forms, with rmsd about 10.7 Å. The shaded rectangle in the upper right corner demonstrates convergence of the two trajectories to the same bent state. The values above 4 Å are not shaded whereas in the darkest zones it falls down to 1.3 Å. The black vertical band at approximately 10 ns indicates that At-A briefly visited the final state 3 ns before the definite transition.

two DNA forms are qualitatively different as regards hydration of grooves and binding of counterions [57–59]. For our purposes, however, these differences are not essential because the minimal B-DNA model is not expected to give stable A-DNA structures and we do not even try to equilibrate the initial A-DNA states. The start from the A form is important because it provides an independent dynamic assay with a very different entry to the B-DNA family, which allows one to verify convergence of trajectories to specific conformations. We analyze separately two levels of structural convergence.

1. Overall shapes

The rmsd comparison between At-A and At-B is shown in Fig. 5. It clearly demonstrates that At-A and At-B trajectories managed to come very close to each other even though their starting points were significantly separated in conformational space. The initial rmsd of 10.7 Å between the canonical 35-mer A- and B-DNA forms eventually went down to as low as 1.3 Å. The final fall of the rmsd occurred when the curvature drastically increased (compare Figs. 2 and 5). Moreover, during the last nanoseconds the bending direction was virtually identical in At-A and At-B and essentially fixed at around 90° [see Fig. 4(b)], which explains the origin of the black rectangle in the upper right corner of Fig. 5. This direction corresponds to bending toward the minor groove at approximately three base pair steps from the middle GC pair [see Fig. 4(a)], that is, at the 3′ end of the third A tract in Fig. 1.

The nAt trajectories exhibited qualitatively different features. The rmsd comparison of any two long intervals of nAt-A and nAt-B gives fluctuations between 3 and 6 Å without any clear time trend. Figure 2 shows that the rmsd from B-DNA also fluctuated between 3 and 6 Å and that it corre-

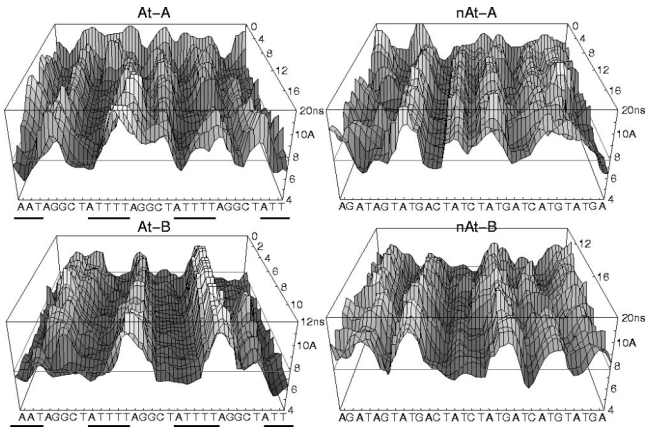

FIG. 6. The time evolution of the profile of the minor groove in the four trajectories. The surface plots are formed by time-averaged successive minor groove profiles, with that on the front face corresponding to the final DNA conformation. The groove width is evaluated by using space traces of C5′ atoms [95]. Its value is given in angströms and the corresponding canonical B-DNA level of 7.7 Å is marked by the thin straight lines on the faces of the box. The sequences are shown for the corresponding top strands in Fig. 1 with the 5′ ends on the left. The A tracts are underlined. Note that the groove width can be measured only starting from the third base pair from both termini.

lated with bending parameters. As seen in Fig. 3 the molecule really was not straight. According to Fig. 4(b) the bending directions in nAt-A and nAt-B were well defined but slightly different. They neither diverged nor converged, remaining at around 100° from each other. The molecule shows no signs of slow straightening, which would give a decrease of fluctuations in Fig. 2 and an increase in scattering of directions in Fig. 4(b). All this suggests that bent shapes are favored over straight ones, and that there are many stable bends, with transitions between them being too rare to be sampled by our simulations.

2. Groove profiles and local structures

The dynamics of the minor groove profiles is shown in Fig. 6. There are evident qualitative resemblance as well as some subtle differences between these four surfaces. In At-B, the characteristic regular groove shape has established early, with significant widenings in the three zones between the A tracts. The far left widening is somewhat different probably because it occurs between antiparallel A tracts. In At-A, the profile strongly changed at the beginning, but also established itself by the end of the tenth nanosecond. Although the final At-A and At-B profiles are not identical, they are clearly similar, with good correspondence of local widenings and narrowings.

The two nAt surfaces show little similarity with each other, but qualitatively their shapes are not very different from those for the A-tract fragment, with modulations of similar wavelengths and amplitudes. This looks somewhat counterintuitive because, in experiments, regular oscillations of the minor groove widths are observed only in A-tract repeats [28], and this structural periodicity is certainly related to that of the sequence. However, such behavior is exactly what one should expect if the waving of the backbone results from its intrinsic compression. In this case, the groove modulations should occur regardless of the base pair sequence and their characteristic wavelengths should be determined by the backbone stiffness as well as overall helical pitch and diameter. This explains why the waves in the left-hand and the right-hand plates in Fig. 6 have roughly similar scales, even though only the A-tract sequence is periodical. In experiment, however, such modulations can be observed only if their phases are fixed in time, which is the case of A-tract repeats. For random sequences, like the one we use as a reference, the fine structure should be smoothed out on averaging over the whole ensemble.

Figure 7 compares B_I/B_{II} backbone dynamics in the two At trajectories. There are many similarities in dynamics as well as in the final configurations. The convergence is better near both ends and within A tracts. The dissimilar distributions of the conformers in the middle correspond to the difference in minor groove profiles in Fig. 6. In A tracts, the B_{II} conformers are very rare in T strands and tend to alternate with B_I in A strands. Figure 8 compares local helical parameters in the last average structures. Only the buckle and propeller traces exhibit large scale modulations phased with the helical screw. All parameters strongly fluctuate with dissimilar phases in the two structures. As earlier [25,51], the fine profiles in Fig. 8 only slightly changed between consecutive nanoseconds, and dissimilar fluctuations were also observed in quenched local minimum energy structures.

3. Coupling between the levels

Figures 4 and 5 demonstrate that At-A and At-B arrived at the same statically bent state. This dynamics contrasts with those of the two nAt trajectories and it strongly suggests that the curved DNA shape of the A-tract fragment is an attractor of trajectories with a metabasin of attraction comprising both canonical A and B DNA forms. Figures 6–8 show that the bending convergence is accompanied by some clear trends in local conformational dynamics. These local features are probably coupled to bending; however, a close look reveals that this coupling is very loose. The convergence of the minor groove profiles in Fig. 6 is at best qualitative. Figure 7 indicates that active backbone dynamics continued after the curvature established itself and that one can pick up rather different distributions of conformers from the ensemble of bent structures. The noisy traces in Fig. 8 obtained by averaging over two similarly bent ensembles suggest that the helical parameters are far from being fixed by bending. The natural conclusion follows that convergence of the bending dynamics does not require unique specific local conformations, i.e., that the bent state is microheterogeneous.

D. The magnitude and the character of bending in the A-tract repeat

The experimental magnitude of bending caused by A tracts was earlier estimated by several groups with different approaches [21,30,60,61]. The reported bend angles were between 11° and 28° per A tract, and 18° is presently consid-

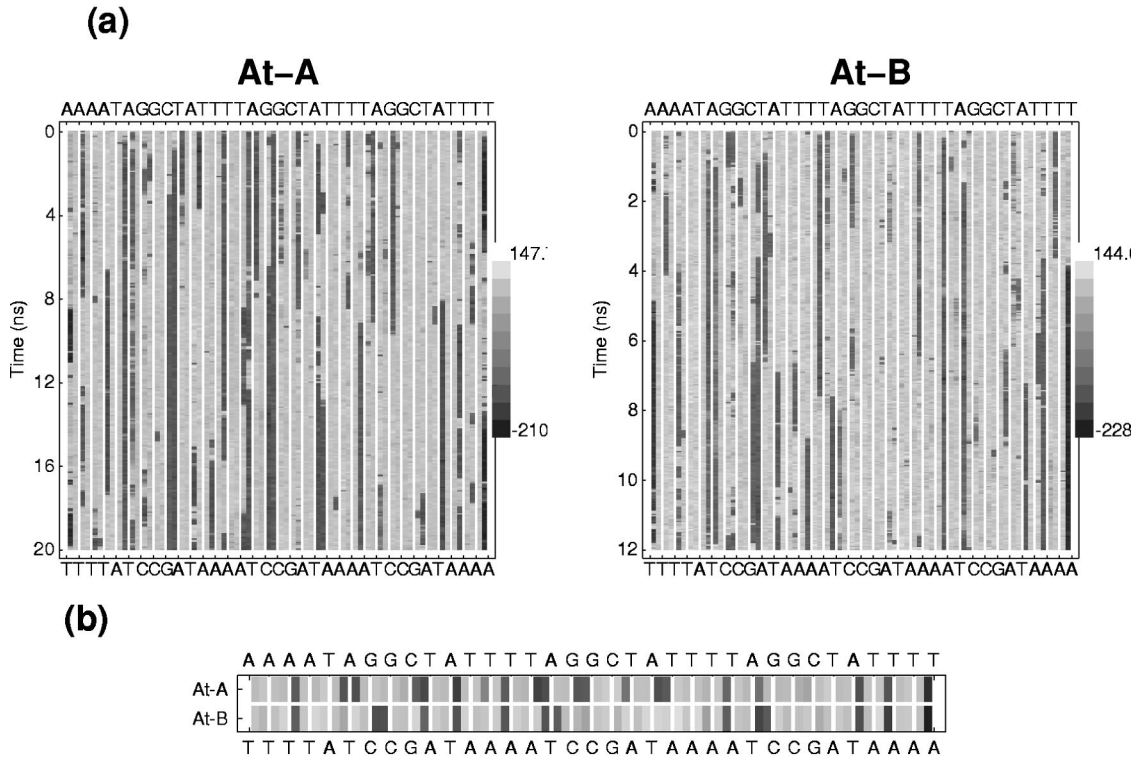

FIG. 7. (a) Dynamics of B_I and B_{II} backbone conformers in At-A and At-B. The B_I and B_{II} conformations are distinguished by the values of two consecutive backbone torsions ε and ζ. In a transition, they change in concerte from (t,g^-) to (g^-,t). The difference $\zeta-\varepsilon$ is, therefore, positive in the B_I state and negative in B_{II}, and it is used as a monitoring indicator, with the corresponding gray scale levels shown on the right. Each base pair step is characterized by a column consisting of two subcolumns, with the left subcolumns referring to the sequence written at the top in the 5′-3′ direction from left to right. The right subcolumns refer to the complementary sequence shown at the bottom. (b) Comparison of the final distributions of B_I and B_{II} backbone conformers in At-A and At-B shown in the same way as in plate (a).

ered as the most reasonable estimate [9]. The curvature somewhat varies with the base pair sequence and depends upon environmental conditions such as the temperature, the concentration of counterions, etc. Although in calculations all these details cannot yet be properly taken into account a quantitative comparison with experiment is instructive.

When the curvature established itself, that is, after 13 ns of dynamics in At-A and after 3 ns in At-B, the bend angle oscillated around 60° (see Fig. 2). In the consecutive 1 ns averaged conformations its value was between 42° and 74°, with the average of 54° for 16 such structures. This value corresponds to $54/4=13.5°$ per A tract, that is, close to the lower experimental estimate. A larger value of $54/3=18°$ results, however, if one assumes, as suggested by some experimental observations [23,62], that the A tracts are straight, and that the bending actually occurs in the three zones between them. Yet another estimate is obtained from the increase of bending with respect to the shorter 25-mer fragment studied earlier [25]. It appears that one additional A tract and junction zone increase the overall bend by $(20–22)°$. We see that the magnitude of bending in simulations is rather close to experimental estimates, and that the agreement is better if the curvature is really localized in the junction zones between A tracts.

Figure 9 presents a closer look at how the local curvature is distributed in the last 1 ns average structure of At-B. The total bending angle is about 50°. Three zones contribute more than others to the overall bend. The two junctions between A tracts 2, 3, and 4 are bent in an identical direction which is close to that of the whole structure. Together they contribute around 40° to the total bend, which is the largest local positive contribution. In contrast, the strongly curved fourth A tract makes a negative contribution because its direction diverges by more than 90°. The third A tract is virtually straight. Finally, A tracts 1 and 2 and the junction zone between them exhibit a smooth curvature with a stable ''good'' direction and contribute the remaining 20° of the total bend.

The foregoing analysis certainly is not free from pitfalls. For instance, the apparent smooth curvature can result from time averaging of several alternative local bends. Nevertheless, Fig. 9 indicates that there are zones in this DNA fragment that are bent more than others and that two such zones are distinguishable between A tracts. Figure 9(c) displays the local bending dynamics in At-B. It is seen that the main features noticed in plates (a) and (b) were quite visible during the whole trajectory. Moreover, the zone between the first two A tracts also sometimes carried an increased curvature. However, it would be incorrect to conclude that A tracts are straight. They just exhibit generally smaller and more distributed curvature than the junction zones. This curvature is usually directed toward the minor groove; therefore it does not cancel out in averaged structures.

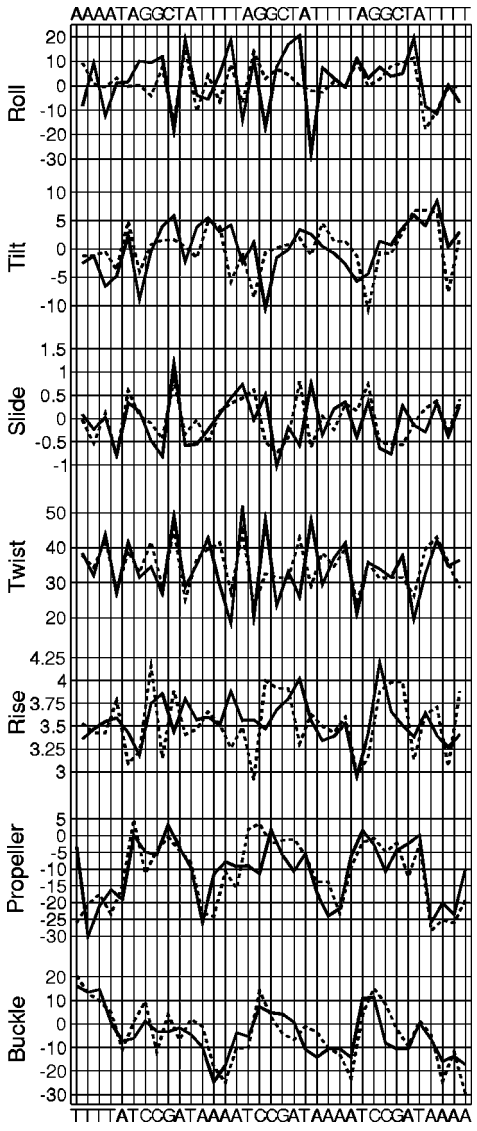

FIG. 8. Sequence variations of helicoidal parameters in the last 1 ns average structures of At-A and At-B. The sequence of the first strand is shown on the top in the 5′-3′ direction. The complementary sequence of the second strand is written on the bottom in the opposite direction. All parameters were evaluated with the CURVES program [49] and are given in degrees and angströms. At-A, solid line; At-B, dashed line.

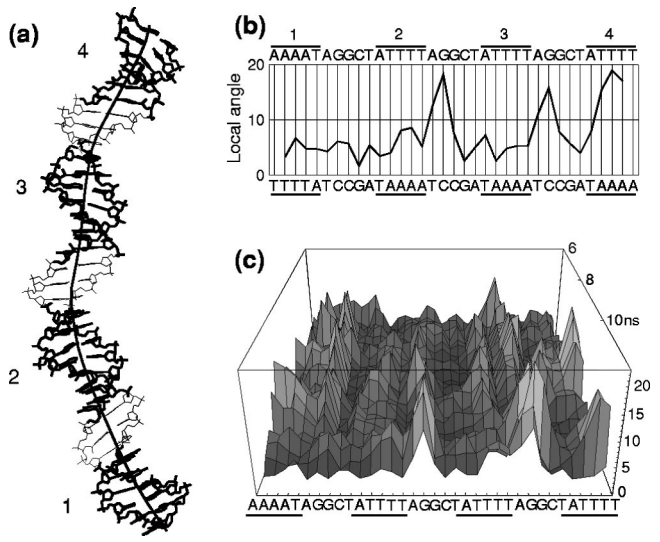

FIG. 9. (a) The last 1 ns average structure of At-B shown in the *XOZ* projection according to Fig. 4(a). The AT base pairs are highlighted. (b) The quantified distribution of curvature in the structure shown in plate (a). The local bending angle is evaluated by moving a sliding window along the helical axis. The window size was 3 base pair steps, with the measured values assigned to its center. The sequences of strands are given as in Fig. 1 with the A tracts underlined and numbered. (c) Dynamics of local bending in At-B. The surface plot is formed by time-averaged successive profiles like that in plate (b), with the front face of the box corresponding to the end of the trajectory.

The foregoing pattern agrees qualitatively with the recent NMR [63] and x-ray data [64] as well as the character of bending earlier observed in calculations [29,37]. Many earlier reported x-ray structures of A tracts suggested that they produce an intrinsically straight DNA compared to other sequences [62]. Our calculations do not contradict these observations because the crystal A-tract structures should be additionally straightened due to special crystallization conditions [65–67], and because a single short A tract may in fact be somewhat less curved than that inserted in a long DNA fragment.

E. Verification of curvature by gel electrophoresis

The sequence induced static DNA curvature was first noticed owing to reduced migration rate of curved DNA fragments in gel electrophoresis [1]. Later gel migration studies provided a wealth of information on curvature in A-tract repeats [7]. The difference in gel mobility between straight and curved DNA rapidly grows with chain length; therefore, the curvature was usually studied in rather long DNA fragments. Data for sequences shorter than 50 bp are rare [68], and, to our best knowledge, it has never been shown that curved and straight 35-mers could be distinguished. As regards the bend direction, it can be determined experimentally only in much longer chains [69]. However, considering the possibility of insertion of the constructed 35-mer fragments into a long stretch of straight DNA, we preferred to use exactly identical fragments in both simulations and experiments. Subtle sequence effects in double stranded oligomers of around 10 bp were detected with higher gel concentration [70], and one could hope that this would work for somewhat longer sequences as well.

Figure 10 shows a comparison of the acrylamide gel mobility of these two fragments. As expected, the A-tract repeat exhibits a reduced rate of migration. The difference is quite significant so that the two molecules are well resolved both in separate lanes and when mixed in the same sample. Owing to the identical base pair content, the effect of factors such as the number of tightly bound counterions and water molecules is reduced here to the minimum, and, most probably, the observed difference is entirely due to the curvature in the A-tract fragment.

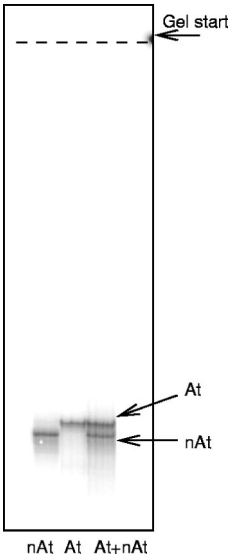

FIG. 10. Gel mobility assay. The two ^{32}P-labeled 35 bp DNA constructs (At and nAt) underwent electrophoresis in 16% plyacrylamide gel buffered with Tris-borate, pH 8.6. The gel was dried and autoradiographed. The lanes labeled At, nAt, and At+nAt correspond to the A-tract repeat, the random sequence, and their mixture, respectively. Bands assigned to each DNA fragment are marked by arrows.

IV. DISCUSSION

A. Comparison with earlier studies

To our knowledge, the only earlier successful unbiased simulations aimed at reproducing A-tract induced curvature in DNA were reported by Beveridge and co-workers [29,37]. These simulations were carried out in a full water environment with explicit counterions. The character of the phased A-tract bending appeared oscillatory with a period of at least 3 to 4 ns [37]. Because the duration of trajectories was only 5 ns, it was difficult to confirm the static character of bending and distinguish between essential and occasional observations. Therefore, conclusions concerning the applicability of different models were not restrictive and left room for many theories. Our simulations have the same goal and a similar setup, but we use a simpler model system. The primarily long term interest in B-DNA models with implicit or semi-implicit representation of environment is connected with approximate simulations of very long DNA molecules [36]. As shown here the minimal model can also capture, at least qualitatively, important sequence effects like the A-tract induced curvature.

Several features in our calculations correspond well to those observed earlier, notably, spontaneous development of quasisinusoidal minor groove profiles in both A-tract and non-A-tract sequences and strong bends in junction zones between A tracts. In contrast to earlier simulations, however, the curvature here emerged after several nanoseconds of dynamics and the difference between the A-tract and non-A-tract structures did not reduce with time, which made possible verification of the attracting property of the bent state. One should note also that the model we use was borrowed from earlier theoretical studies with no specific fitting for A tracts [47], and yet A-tract structures computed here are very close to experimental data as regards the helical pitch and the absolute groove sizes [25]. In standard AMBER and CHARMM simulations, B-DNA always appears somewhat underwound and the narrowest A-tract minor grooves remain 1–2 Å wider than in experimental structures [29,37,39]. The origin of this subtle bias remains unclear, and attempts to reduce it have been made in the very recent modifications of the AMBER force field [44,71].

The small experiment included in the present report is similar to earlier extensive gel migration studies of DNA bending; nevertheless, it involves a few different features. To our knowledge, this is the first case when the gel mobility of an A-tract DNA fragment is compared with that of a *random* sequence with *identical base pair composition*. The 35-mer DNA fragments are shown to be separable in gels. Finally, the same DNA fragments are compared *in silico* and *in vitro*. This small experiment certainly cannot prove the correctness of our simulations and theoretical conclusions, but it agrees with them. All this represents a significant enforcement of the present results compared to our previous reports [25,51], which became possible owing to the increased DNA length. Parallel investigation of 35–50 bp DNA fragments in simulations and gel migration experiments is an attractive general approach to sequence effects and we continue our efforts in this direction.

B. Comparison with theories of DNA bending

The origin of intrinsic curvature in DNA remains unclear. Theories that explain it always assume some specific balance of interactions in the DNA structure, and that is why these theories are perhaps more important than the particular role of A tracts. The list of available interactions is well known, but the question is which of them is the driving force. Below we briefly analyze our results in the contexts of some theories.

1. Base pair stacking models

According to any mechanism that starts from base pair stacking, like the wedge or the junction models [2,12,18], a curved DNA molecule must be built out of asymmetric blocks, with their structures determined by base pair sequence. The bending, therefore, must be accompanied by repetition of local structures in identical sequence fragments. This fundamental theoretical prediction fails for the static bends observed here, which confirms earlier conclusions [25,51]. The structures of sequence repeats in the bent state are microscopically heterogeneous and convergence to specific local conformations is not necessary for bending. As shown above, the A-tract trajectories arrive at a single bent state, but the minor groove profiles in Fig. 6 are only similar, not identical, like the local helical parameters and backbone conformations in Figs. 7 and 8.

2. Counterion electrostatic models

An alternative model that recently attracted much attention considers solvent cations trapped in A-tract minor grooves as the initial cause of bending [24]. The role of

counterions in this phenomenon is rather controversial [64,72,73], and a few general comments are necessary before considering our results. Because straight DNA structures correspond to symmetric minima of electrostatic energy bends can result from symmetry breaking in the charge distribution, namely, if positive external charges accumulate at one DNA side it should bend toward them [24,74–77]. However, the same situation is well interpreted by other models of bending; namely, in a curved double helix, the phosphate groups at the inner edge must approach, which creates regions of low potential that should be populated by counterions if they are available [60]. Here the counterion-DNA interactions are structure specific and they stabilize preexisting curvature while in the electrostatic models the counterions recognize the sequence rather than the overall bend structure and they cause the curvature.

Two physically different electrostatic models can be distinguished. In the first one the counterions act locally. When a counterion is placed in one of the DNA grooves between two phosphate groups their electrostatic interaction becomes attractive, which narrows the groove [77]. As in some earlier models [26,28], the global curvature results from a general mechanical link between groove deformations and bending. In contrast, the second model is purely electrostatic. Here the minor grooves of A tracts act as flexible ionophores [24,78] and trap counterions. Since in phased sequences these ''traps'' occur at the same DNA side the double helix bends toward them to relax the long range phosphate repulsion at the opposite side.

The first model cannot explain the origin of the A-tract curvature because only multivalent counterions can cause significant bends [77] whereas bending is commonly observed in buffers containing EDTA and other chelating agents. Also, the optimal counterion position for this type of bend is at the entrance of the groove and not inside; therefore, it cannot be both strong and sequence specific. The last argument agrees with the recent MD studies of correlations between the minor groove width and positioning of counterions. Notably, there is no such correlation when only counterions interacting with bases are considered [73]. In contrast, a correlation exists for counterion positions at the groove entrance [79]. The last observation corresponds to the structure specific binding better than to the sequence specific one. Structure specific interactions can explain all experimental results concerning the preferential binding of counterions in A tracts [24,80,81], which makes such data intrinsically neutral as regards different models of bending.

The second model employs the general idea initially proposed for protein-DNA interactions [74] and confirmed experimentally for free DNA [75]. However, it qualitatively disagrees with a cornerstone experimental observation concerning the A-tract induced bending, namely, that an A tract can be characterized by a definite bend angle regardless of its length and the distance from other A tracts. When the length of an A tract exceeds one helical turn, both sides of the double helix appear neutralized. As a result, the curvature should decrease in the series $(A_{12}N_9)_n$-$(A_{14}N_7)_n$-$(A_{16}N_5)_n$ because the length of the non-neutralized N tracts is reduced, and furthermore in the sequence $(A_{16}N_5)_n$ the bend angle per A tract should be drastically reduced with respect to that in $(A_6N_5)_n$, for example, because the distance between the repulsive N tracts is increased. These predictions apparently disagree with the experimental trends [82] although additional experiments are perhaps necessary to check them.

In our calculations all counterion effects are considered nonspecific, and the results obtained indicate that modulations of DNA grooves and static bending are physically possible without breaking the charge symmetry around DNA. Although simulations alone cannot prove the real mechanism all experimental and computational observations taken together suggest that solvent counterions are hardly responsible for the intrinsic curvature in DNA, which by no means calls into question their important role in DNA structure and function.

3. Compressed backbone theory

This theory considers the ideal B-DNA structure as consisting of a straight cylindrical core formed by stacked base pairs and two threads of sugar-phosphate backbone that go along two parallel spiral traces on its surface. The core is around 10 Å in diameter and the threads are attached to it at the N_1/N_9 atoms of pyrimidines and purines, respectively. The threads have a number of conformational degrees of freedom that participate in thermal motion; therefore, they should be treated as charged polymer chains partially immobilized on a cylindrical surface and characterized by a certain equilibrium specific length. On the other hand, the distance between the consecutive $N_{1/9}$ atoms is determined by the core diameter, the twist angle, and the rise between consecutive base pair planes. The question is how well these $N_{1/9}$ distances correspond to the optimal polymer length of the backbone threads.

Since the discovery of the double helix it is always drawn as a straight rod with a regular spiral backbone. Because the spiral trace is the shortest line that joins two points on a cylindrical surface this model, in fact, tacitly implies that the backbone is stretched and tends to shrink. Imagine, as postulated by the compressed backbone theory, that the preferred backbone length is longer than that in the canonical B-DNA and that it tries to extend by pushing bases. The extension can be accommodated by increasing the twist angle, for instance, which, however, is opposed by the loss in the stacking energy. When it becomes difficult to extend in this way, the backbone will tend to deviate from the ideal spiral trace. The two backbone threads become nonparallel, with the widths of the two double helix grooves forced to vary. The parallel stacking has to be perturbed, which can induce local bending in directions determined by widenings and narrowings of the minor groove [25]. In fact, the origin of bending in this model is qualitatively similar to that in a straight elastic rod exposed to a torsional deformation, with the small difference that, in a linear DNA, the torsional stress upon the backbone comes from the core of the structure.

The above correspondence of lengths can hardly be checked directly by molecular mechanics calculations. Because of the polymer flexibility and the charges at phosphate groups this system should be very sensitive to the local microscopic environment, which is indicated by numerous ex-

perimental observations. Note, for instance, that the A-tract curvature is drastically reduced if the temperature is increased beyond 40 °C [86], when the overall DNA structure does not yet change according to all other tests available. Nevertheless, there are a few independent experimental facts, not necessarily related directly to bending, that support the compressed backbone state. For instance, smooth groove modulations are ubiquitous in all x-ray B-DNA structures obtained until now, which is an immediate indicator of a compressed backbone. The temperature effects are also explained specifically, which distinguished this theory from other models of DNA bending; namely, since the backbone is a charged polymer its equilibrium specific length is maximal at low temperature. With growing temperature, the average length is reduced due to thermal fluctuations, which should cause reduction of intrinsic curvature regardless of the sequence, as observed in experiments [86].

The compressed backbone theory predicts that smooth modulations of DNA grooves should appear spontaneously with any base pair sequence. The helical symmetry becomes broken with the base pair stacking perturbed, which creates regions of intrinsic curvature. In a ''random'' DNA, the local curvature changes its direction with time because groove widenings and narrowings migrate slowly along the double helix. As a result, the generic DNA appears straight on average although it is curved locally. In sequences where certain base pair properties strongly alternate, the phases of backbone oscillations appear fixed. In this case the local curvature can sum up to give macroscopic static bends, as in many periodical sequences of which A-tract repeats represent the most beautiful example [14].

The competition between the stacking interactions and the backbone compression postulated by this theory is characteristic of physical systems said to be frustrated [90]. Consider the common textbook example of three antiferromagnetic spins in a triangle configuration. The optimal orientation of each pair is antiparallel, but all three pairs cannot be antiparallel in a triangle. There is always at least one parallel pair and the ground state appears degenerate. Now consider a circular duplex DNA with a homopolymer sequence. The compressed backbone causes groove modulations, but there are no preferable regions for narrowings and widenings and the ground state appears strongly degenerate. The similarity between these two examples is evident. In contrast, in periodical A-tract repeats, frustration is relieved because the A tracts mark zones where the minor groove can be easily narrowed since larger propeller and helical twists are allowed. One usual physical consequence of frustration is very important for biology, namely, the possibility of a glassy state where microscopic transitions are dramatically slowed down. Transitions between wavy backbone configurations in a long DNA can be very slow because many groove narrowings and widenings must be moved in concert. This may explain experimental observations of very slow relaxation dynamics in relatively short DNA fragments [55,56,91].

The above views offer a different interpretation of some seemingly strange environmental effects upon the curvature. Common physical factors like the temperature, counterions, and various dehydrating agents are long known to slightly change the helical pitch of DNA [83–85], which can reasonably be attributed to the dependence of the state of the DNA backbone upon the solvent screening of phosphates. These same factors significantly modulate the sequence specificity of nucleases, probably by changing the shape of DNA grooves [27], and produce complex effects upon the intrinsic curvature [65,66,68,86–89]. It seems wise to postpone any detailed interpretation of these facts for future studies, but one can just note that with the intrinsic frustration outlined above a very small change in the partial specific backbone length can induce significant global changes in the DNA structure.

It is clear from all the above discussion that the compressed backbone hypothesis agrees with our computational results, and it is the only such theory presently available. It considers a macroscopically curved DNA as an ''idioform'' characterized by topological attributes, rather than a structure with fixed atom positions. Therefore, the microheterogeneity of the bent state should be expected because the same waving backbone profile is compatible with many alternative local conformations.

C. Possibilities of experimental verification of backbone compression

According to the compressed backbone theory, local sequence specific stacking in B-DNA is put into a medium range context imposed by backbone modulations. Therefore, no simple rules exist for *a priori* calculation of curvature in any sequence, and predicting the fine structure for DNA appears as difficult as for proteins, for instance. Nevertheless, there are some qualitative predictions that can be checked in experiments. This theory suggests, for example, that the A-tract curvature can be relaxed by introducing single-stranded breaks (nicks). To check this suggestion one has to examine the gel mobility of A-tract DNA fragments containing such breaks in different positions. Since the backbone compression should increase in minor groove widenings between A tracts [25], these are sites where single stranded breaks are most likely to relax the curvature. In contrast, the conventional view of the DNA structure suggests that such DNA fragments always look identical in gels.

It is also interesting to examine the possible relationship between the backbone compression and supercoiling. There is a consensus that intrinsic bends affect the shape of the superhelical DNA [92,93]. Unlike other models, however, the compressed backbone theory predicts that the intrinsic curvature should vary under superhelical stress in a rather special way; namely, with a positive density, the backbone is stretched and the curvature of an internal A-tract repeat should be reduced. Conversely, the curvature should increase when the superhelical density is negative. Diekmann and Wang earlier observed that the A-tract structure changes under superhelical stress [86], and their approach may serve for a more specific experimental verification of the above theoretical predictions. These predictions can also be checked directly by electron microscopy of plasmids with internal A tracts under small positive and negative superhelical stress.

[1] J.C. Marini, S.D. Levene, D.M. Crothers, and P.T. Englund, Proc. Natl. Acad. Sci. U.S.A. **79**, 7664 (1982).
[2] H.-M. Wu and D.M. Crothers, Nature (London) **308**, 509 (1984).
[3] P.J. Hagerman, Proc. Natl. Acad. Sci. U.S.A. **81**, 4632 (1984).
[4] S. Diekmann, in *Nucleic Acids and Molecular Biology*, Vol. 1, edited by F. Eckstein and D.M.J. Lilley (Springer-Verlag, Berlin, 1987), pp. 138–156.
[5] P.J. Hagerman, Annu. Rev. Biochem. **59**, 755 (1990).
[6] D.M. Crothers, T.E. Haran, and J.G. Nadeau, J. Biol. Chem. **265**, 7093 (1990).
[7] D.M. Crothers and J. Drak, Methods Enzymol. **212**, 46 (1992).
[8] W. K. Olson and V. B. Zhurkin, in *Structure and Dynamics. Vol. 2: Proceedings of the Ninth Conversation, State University of New York, Albany, N.Y. 1995*, edited by R. H. Sarma and M. H. Sarma (Adenine Press, New York, 1996), pp. 341–370.
[9] D. M. Crothers and Z. Shakked, in *Oxford Handbook of Nucleic Acid Structure*, edited by S. Neidle (Oxford University Press, New York, 1999), pp. 455–470.
[10] N.Z. Namoradze, A.N. Goryunov, and T.M. Birshtein, Biophys. Chem. **7**, 59 (1977).
[11] V.B. Zhurkin, Y.P. Lysov, and V.I. Ivanov, Nucleic Acids Res. **6**, 1081 (1979).
[12] E.N. Trifonov and J.L. Sussman, Proc. Natl. Acad. Sci. U.S.A. **77**, 3816 (1980).
[13] P. De Santis, A. Palleschi, M. Savino, and A. Scipioni, Biochemistry **29**, 9269 (1990).
[14] A. Bolshoy, P. McNamara, R.E. Harrington, and E.N. Trifonov, Proc. Natl. Acad. Sci. U.S.A. **88**, 2312 (1991).
[15] Y. Liu and D.L. Beveridge, J. Biomol. Struct. Dyn. **18**, 505 (2001).
[16] M. Dlakić and R.E. Harrington, Proc. Natl. Acad. Sci. U.S.A. **93**, 3847 (1996).
[17] M. Dlakić and R.E. Harrington, Nucleic Acids Res. **26**, 4274 (1998).
[18] S.D. Levene and D.M. Crothers, J. Biomol. Struct. Dyn. **1**, 429 (1983).
[19] E. Selsing, R.D. Wells, C.J. Alden, and S. Arnott, J. Biol. Chem. **254**, 5417 (1979).
[20] D.G. Alexeev, A.A. Lipanov, and I.Y. Skuratovskii, Nature (London) **325**, 821 (1987).
[21] C.R. Calladine, H.R. Drew, and M.J. McCall, J. Mol. Biol. **201**, 127 (1988).
[22] R.C. Maroun and W.K. Olson, Biopolymers **27**, 585 (1988).
[23] R.E. Dickerson, D.S. Goodsell, and S. Neidle, Proc. Natl. Acad. Sci. U.S.A. **91**, 3579 (1994).
[24] N.V. Hud, V. Sklenář, and J. Feigon, J. Mol. Biol. **286**, 651 (1999).
[25] A.K. Mazur, J. Am. Chem. Soc. **122**, 12 778 (2000).
[26] H.R. Drew and A.A. Travers, J. Mol. Biol. **186**, 773 (1985).
[27] H.R. Drew and A.A. Travers, Cell **37**, 491 (1984).
[28] A.M. Burkhoff and T.D. Tullius, Cell **48**, 935 (1987).
[29] D. Sprous, M.A. Young, and D.L. Beveridge, J. Mol. Biol. **285**, 1623 (1999).
[30] H.-S. Koo, J. Drak, J.A. Rice, and D.M. Crothers, Biochemistry **29**, 4227 (1990).
[31] N.B. Ulyanov and V.B. Zhurkin, J. Biomol. Struct. Dyn. **2**, 361 (1984).
[32] S.R. Sanghani, K. Zakrzewska, S.C. Harvey, and R. Lavery, Nucleic Acids Res. **24**, 1632 (1996).
[33] E. von Kitzing and S. Diekmann, Eur. Biophys. J. **14**, 13 (1987).
[34] V.P. Chuprina and R.A. Abagyan, J. Biomol. Struct. Dyn. **6**, 121 (1988).
[35] V.B. Zhurkin, N.B. Ulyanov, A.A. Gorin, and R.L. Jernigan, Proc. Natl. Acad. Sci. U.S.A. **88**, 7046 (1991).
[36] T.E. Cheatham III and P.A. Kollman, Annu. Rev. Phys. Chem. **51**, 435 (2000).
[37] M.A. Young and D.L. Beveridge, J. Mol. Biol. **281**, 675 (1998).
[38] E.C. Sherer, S.A. Harris, R. Soliva, M. Orozco, and C.A. Laughton, J. Am. Chem. Soc. **121**, 5981 (1999).
[39] D. Strahs and T. Schlick, J. Mol. Biol. **301**, 643 (2000).
[40] A.K. Mazur, J. Comput. Chem. **18**, 1354 (1997).
[41] A.K. Mazur, in *Computational Biochemistry and Biophysics*, edited by O.M. Becker, A.D. MacKerell, Jr., B. Roux, and M. Watanabe (Marcel Dekker, New York, 2001), pp. 115–131.
[42] A.K. Mazur, J. Chem. Phys. **111**, 1407 (1999).
[43] W.D. Cornell, P. Cieplak, C.I. Bayly, I.R. Gould, K.M. Merz, D.M. Ferguson, D.C. Spellmeyer, T. Fox, J.W. Caldwell, and P.A. Kollman, J. Am. Chem. Soc. **117**, 5179 (1995).
[44] T.E. Cheatham III, P. Cieplak, and P.A. Kollman, J. Biomol. Struct. Dyn. **16**, 845 (1999).
[45] W.L. Jorgensen, J. Am. Chem. Soc. **103**, 335 (1981).
[46] A.K. Mazur, J. Am. Chem. Soc. **120**, 10 928 (1998).
[47] A.K. Mazur, J. Comput. Chem. **22**, 457 (2001).
[48] S. Arnott and D.W.L. Hukins, Biochem. Biophys. Res. Commun. **47**, 1504 (1972).
[49] R. Lavery and H. Sklenar, J. Biomol. Struct. Dyn. **6**, 63 (1988).
[50] P. Tuffery, J. Mol. Graphics **13**, 67 (1995).
[51] A.K. Mazur, J. Biomol. Struct. Dyn. **18**, 832 (2001).
[52] H.-S. Koo, H.-M. Wu, and D.M. Crothers, Nature (London) **320**, 501 (1986).
[53] W. Kabsch, C. Sander, and E.N. Trifonov, Nucleic Acids Res. **10**, 1097 (1982).
[54] W.K. Olson, N.L. Marky, R.L. Jernigan, and V.B. Zhurkin, J. Mol. Biol. **232**, 530 (1993).
[55] L. Song and J.M. Schurr, Biopolymers **30**, 229 (1990).
[56] T.M. Okonogi, A.W. Reese, S.C. Alley, P.B. Hopkins, and R.H. Robinson, Biophys. J. **77**, 3256 (1999).
[57] R. Lavery and B. Pullman, Nucleic Acids Res. **9**, 4677 (1981).
[58] N. Pattabiraman, R. Langridge, and P.A. Kollman, J. Biomol. Struct. Dyn. **1**, 1525 (1984).
[59] W. Saenger, W.N. Hunter, and O. Kennard, Nature (London) **324**, 385 (1986).
[60] S.D. Levene, H.-M. Wu, and D.M. Crothers, Biochemistry **25**, 3988 (1986).
[61] L.E. Ulanovsky, M. Bodner, E.N. Trifonov, and M. Choder, Proc. Natl. Acad. Sci. U.S.A. **83**, 862 (1986).
[62] M.A. Young, G. Ravishanker, D.L. Beveridge, and H.M. Berman, Biophys. J. **68**, 2454 (1995).
[63] D. MacDonald, K. Herbert, X. Zhang, T. Polgruto, and P. Lu, J. Mol. Biol. **306**, 1081 (2001).
[64] T.K. Chiu, M. Zaczor-Grzeskowiak, and R.E. Dickerson, J. Mol. Biol. **292**, 589 (1999).
[65] D. Sprous, W. Zacharias, Z.A. Wood, and S.C. Harvey, Nucleic Acids Res. **23**, 1816 (1995).

[66] M. Dlakic, K. Park, J.D. Griffith, S.C. Harvey, and R.E. Harrington, J. Biol. Chem. **271**, 17911 (1996).
[67] R.E. Dickerson, D. Goodsell, and M.L. Kopka, J. Mol. Biol. **256**, 108 (1996).
[68] S. Diekmann, Nucleic Acids Res. **15**, 247 (1987).
[69] S.S. Zinkel and D.M. Crothers, Nature (London) **328**, 178 (1987).
[70] J.-H. Chen, N.C. Seeman, and N.R. Kallenbach, Nucleic Acids Res. **16**, 6803 (1988).
[71] J. Wang, P. Cieplak, and P.A. Kollman, J. Comput. Chem. **21**, 1049 (2000).
[72] L. McFail-Isom, C.C. Sines, and L.D. Williams, Curr. Opin. Struct. Biol. **9**, 298 (1999).
[73] K.J. McConnell and D.L. Beverdige, J. Mol. Biol. **304**, 803 (2000).
[74] A.D. Mirzabekov and A. Rich, Proc. Natl. Acad. Sci. U.S.A. **76**, 1118 (1979).
[75] J.K. Strauss and L.J. Maher III, Science **266**, 1829 (1994).
[76] M.A. Young, B. Jayaram, and D.L. Beveridge, J. Am. Chem. Soc. **119**, 59 (1997).
[77] I. Rouzina and V.A. Bloomfield, Biophys. J. **74**, 3152 (1998).
[78] N.V. Hud and M. Polak, Curr. Opin. Struct. Biol. **11**, 293 (2001).
[79] D. Hamelberg, L.D. Williams, and W.D. Wilson, J. Am. Chem. Soc. **32**, 7745 (2001).
[80] N.V. Hud and J. Feigon, J. Am. Chem. Soc. **119**, 5756 (1997).
[81] N.C. Stellwagen, S. Magnusdottir, C. Gelfi, and P.G. Righetti, J. Mol. Biol. **305**, 1025 (2001).
[82] T.E. Haran and D.M. Crothers, Biochemistry **28**, 2763 (1989).
[83] R.E. Depew and J.C. Wang, Proc. Natl. Acad. Sci. U.S.A. **72**, 4275 (1975).
[84] P. Anderson and W. Bauer, Biochemistry **17**, 594 (1978).
[85] C.-H. Lee, H. Mizusawa, and T. Kakefuda, Proc. Natl. Acad. Sci. U.S.A. **78**, 2838 (1981).
[86] S. Diekmann and J.C. Wang, J. Mol. Biol. **186**, 1 (1985).
[87] B. Jerkovic and P.H. Bolton, Biochemistry **39**, 12 121 (2000).
[88] J.C. Marini, P.N. Effron, T.C. Goodman, C.K. Singleton, R.D. Wells, R.M. Wartell, and P.T. Englund, J. Biol. Chem. **259**, 8974 (1984).
[89] W. Saenger, *Principles of Nucleic Acid Structure* (Springer-Verlag, New York, 1984).
[90] R. Liebmann, in *Statistical Mechanics of Periodic Frustrated Ising Systems*, Lecture Notes in Physics Vol. 251 (Springer, Berlin, 1986).
[91] E.B. Brauns, M.L. Madaras, R.S. Coleman, C.J. Murphy, and M.A. Berg, Phys. Rev. Lett. **88**, 158101 (2002).
[92] C.H. Laundon and J.D. Griffith, Cell **52**, 545 (1988).
[93] Y. Yang, T.P. Westcott, S.C. Pedersen, I. Tobias, and W.K. Olson, Trends Biochem. Sci. **20**, 313 (1995).
[94] R.E. Dickerson, *et al.*, J. Mol. Biol. **205**, 787 (1989).
[95] A.K. Mazur, J. Mol. Biol. **290**, 373 (1999).